On the channel density of EEG signals for reliable biometric recognition

Author:
Wang, Min; Kasmarik, Kathryn; Bezerianos, Anastasios; Tan, Kay Chen; Abbass, Hussein

Publication details:
Pattern Recognition Letters
v. 147
0167-8655 (ISSN); 1872-7344 (ISSN)

Publication Date:
2021

Publisher DOI:
https://doi.org/10.1016/j.patrec.2021.04.003

Research Highlights (Required)

- EEG channel density has an impact on biometric recognition accuracy and inter-state stability.
- A biometric recognition framework that increases EEG channel density improves recognition accuracy and stability.
- Deep neural networks learn effective biometric identifiers for brain biometric applications.

ELSEVIER

Pattern Recognition Letters
journal homepage: www.elsevier.com

On the channel density of EEG signals for reliable biometric recognition

Min Wang[a,**], Kathryn Kasmarik[a], Anastasios Bezerianos[b], Kay Chen Tan[c], Hussein Abbass[a]

[a]*School of Engineering and Information Technology, University of New South Wales, Canberra, ACT 2612, Australia*
[b]*Hellenic Institute of Transport, Center for Research and Technology Hellas, Thessaloniki, Greece.*
[c]*Hong Kong Polytechnic University, Hong Kong SAR, China*

ABSTRACT

Electroencephalography (EEG) provides appealing biometrics by encompassing unique attributes including robustness against forgery, privacy compliance, and aliveness detection. Among the main challenges in deploying EEG biometric systems in real-world applications, stability and availability are two important ones. They respectively reflect the capacity of the system to provide reliable performance within and across different states, and the ease of use of the system. Previous studies indicate that the usability of an EEG biometric system is largely affected by the number of electrodes and reducing channel density is an effective way to enhance usability. However, it is still unclear what is the impact of channel density on recognition performance and stability. This study examines this issue for systems using different feature extraction and classification methods. Our results reveal a trade-off between channel density and stability. With low-density EEG, the recognition accuracy and stability are compromised to varying degrees. Based on the analysis, we propose a framework that integrates channel density augmentation, functional connectivity estimation and deep learning models for practical and stable EEG biometric systems. The framework helps to improve the stability of EEG biometric systems using consumer-grade low channel density devices, while retaining the advantages of high usability.

1. Introduction

EEG is potentially a superior biometric modality as it presents unique attributes not possessed by other modalities such as fingerprints, retina and face scan, in terms of robustness against forgery, privacy compliance, aliveness detection and multi-uses as cognitive biomarkers [1, 2, 3]. Existing research on EEG biometrics has mainly split into two genres, one based on event-related potential (ERP) which is EEG response to a stimulus, and the other based on ongoing EEG which is a spontaneous signal naturally produced by the brain. The ERP biometric system usually tightly controls the cognitive state of the subject through repetitive sensory stimulation and strict signal elicitation protocols. On the contrary, the ongoing EEG biometric system is more flexible in signal acquisition, suitable for unobtrusive and continuous application scenarios, but its stability is relatively poor [2]. The major problems of deploying ongoing EEG biometric systems in real-life scenarios are: the relatively low recognition rate, unstable performance over diverse human states, and human inconvenience during the signal acquisition process due to the discomfort caused by prolonged attachment of electrodes [1]. Previous studies focused more on the theoretical aspects of EEG biometrics, including the elicitation protocols, feature extraction methods, and classification models. This study targets the stability and usability issues which are two key factors towards the practical deployment of EEG biometric systems.

EEG signals are known to be sensitive to mental states, which could generate large intra-subject variations that hinder the recognition accuracy of EEG-based biometric recognition systems. Stability refers to the robustness of the system to mental states and reflects the capacity of the system to provide stable performance within and across different states and tasks. A few recent studies tested the stability of different methods of EEG biometrics in intra-state and inter-state scenarios [4, 5, 2, 6]. Specifically, in the intra-state scenarios, the system is trained and tested on EEG signals collected in the same state or task;

**Corresponding author.
e-mail: `maggie.wang1@adfa.edu.au` (Min Wang)

while in the inter-state scenarios, the system is tested on unseen states that are different from the one used for training. Their results show a significant drop of correct recognition rate (CRR) in the inter-state scenarios, which confirmed the EEG intra-subject variations. In addition, the results show that the set of channels that provide high individual uniqueness changes with the state, which implies that having sufficient channels is important to maintain the stability of EEG biometric systems [5].

On the other hand, the usability of EEG biometrics, which refers to the ease of use of the system, has been increasing in recent years with the development of sensor technology and consumer-grade EEG collection devices which usually have fewer numbers of electrodes compared to clinical-grade devices. Su Yang and Farzin Deravi defined a usability score to evaluate EEG biometric systems [7], i.e., $U = \frac{N \times CRR}{T_r + K \times T_s}$, where K and N denote the number of electrode employed and the number of subjects for which the system was tested on, and T_r and T_s are the recording duration of the training set and test set, respectively. Among these factors, N, T_r, and T_s are experiment-related ones that are adjustable with different setups, while K is a system-related factor which is determined by the methodology and directly affects feature extraction and classification. The equation indicates that the usability of an EEG biometric system is inversely proportional to the number of electrodes employed, therefore, reducing the channel density is an effective way to enhance usability.

From the user's perspective, using low-density EEG facilitates the data collection process, enhances the user experience, and therefore, improves the usability of EEG biometrics. But the impact of channel density on the recognition performance and stability of EEG biometric systems is still an open research question. Therefore, the objectives of this study are two folds, i.e., to evaluate the impact of channel density on CRR and stability of EEG biometric systems that use different feature extraction and classification methods; and if low density does lead to a compromise in CRR and stability, how to enhance the CRR and stability of a low-density system while maintaining its advantages in usability. The following section reviews existing feature extraction and classification methods of EEG biometrics. Section 3 analyses the impact of channel density on biometric recognition performance and stability for different methods. Based on the analysis, a framework integrating density augmentation, functional connectivity, and deep learning model is proposed in Section 4 for practical and reliable EEG biometric recognition systems.

2. Previous work on EEG biometrics

2.1. Feature extraction and selection

Considering different characteristics of EEG signals in the time and frequency domains, many feature extraction methods have been proposed for EEG biometrics, including autoregressive (AR) stochastic modelling [8, 9], Fourier-based power spectral density (PSD) analysis [10], entropy estimation [11] and wavelet packet analysis [4]. Despite the use of different methods, what these features have in common is that they all rely on signals acquired from individual electrodes, which means they do not consider inter-channel information. We refer to this type of feature as univariate features. Univariate features usually work well with ERP signals and EEG signals under resting states. However, their performance decreases significantly with ongoing EEG in diverse states where the subjects' cognitive states are not under strict control [2]. The major reason for the large performance drop is that univariate features are sensitive to the amplitude changes of EEG signals which could lead to considerable intra-subject variations [12]. This is usually inevitable, especially in the case of ongoing EEG signals with weak experimental control. To address this problem, brain connectivity, which considers the dependencies among channels, was proposed for more robust EEG biometrics [10, 2]. While two signals may vary in amplitudes or phases, strong connectivity occurs when their statistical dependence or causal interaction states remains high [13]. This property can help reduce the intra-subject variations and improve biometric performance. So far, several functional connectivity and effective connectivity metrics have been studied for human distinctiveness, including Pearson's correlation [14], spectral coherence [10], and phase synchronisation measures [15, 2, 6]. In addition to using brain connectivity values directly as feature vectors, topological features extracted from brain connectivity networks were also investigated for EEG biometric identifiers [14, 15, 5]. It is worth noting that, for classical methods using univariate features and conventional classifiers, feature selection is usually an important step before classification to enhance the discriminative power of the feature set. In EEG biometrics, recursive feature elimination, information theory based-methods and correlation analysis are often used for feature selection [5].

2.2. Classification and machine learning

Classification is another key element of a biometric recognition system. Although the mainstream for EEG biometrics is still traditional classifiers such as discriminate analysis [9, 4, 14] and similarity measures [10, 8], deep learning has been receiving more and more attention. Compared with traditional classifiers, deep learning shows advantages in extracting identity-bearing information from EEG without feature engineering [16] and offers possibilities to handle large intra-subject variations to support more stable biometrics against diverse human states [2]. Convolutional neural networks (CNN) have shown promising results in learning biometric identifiers from EEG timeseries and functional connectivity networks (FCN), as summarised in Table 1. In most of the studies, the input of CNN was multi-channel EEG or ERP time series (organised in 2-D format) and CNNs were used to learn the morphological characteristics and temporal dependencies from the signal timeseries. However, EEG amplitudes are sensitive to human states and our previous study shows that the direct combination of signal timeseries and CNNs is not able to deal with EEG cross different mental states. This may explain why these studies focus on ERP signals and EEG signals in resting state. A recent study shows that deep learning models integrating functional connectivity are able to provide stable performance with ongoing EEG signals in diverse states [2]. It is worth noting that deep learning methods usually omit the step of feature selection since a deep and hierarchical model itself is capable of extracting high level representations from the input [17].

Table 1: EEG biometric identification using deep learning

Study	Subjects	Channels	States	Inputs	Models	Within-state CRR
[16]	4,10	8	ERP	Raw	CNN	96.8%
[18]	40	17	ERP	ERP	CNN	80.65-98.8%
[19]	10	64	Resting	Raw	CNN	82%
[20]	100	64	Driving simulation	Raw	CNN	97%
[21]	120	64	Resting, ERP	Raw	MLP, CNN, RNN	62.2-92.9%
[2]	109,59	64,46	Diverse	FCN	CNN, GCNN	98.13-99.99%

Deep neural networks are essentially data-driven models and having sufficient data is important for successful training. In terms of having sufficient EEG data, there are two dimensions: signal length and number of channels, which determine the number of training samples and the dimension of each input. Generative models such as generative adversarial networks (GAN) [22] were proposed to augment EEG training samples to improve classification performance. Regularised auto-encoders with proper gate control was proposed to learning relationships between EEG channels, which can be used for missing channel reconstruction [23]. However, there is so far no discussion about the channel density issue, especially the impact of channel density on deep learning-based EEG biometrics.

3. Impact of EEG channel density on biometric recognition

In this section, we examine the impact of EEG channel density on biometric recognition in terms of CRR and stability against varying states. To measure stability, we follow the existing approach that evaluates the method in intra-state condition and inter-state condition. The intra-state condition is to train and test a model using EEG collected in the same state. This condition has been widely adopted in existing research. However, it is insufficient on its own, because it cannot be guaranteed that the cognitive state of a subject during the test phase remains the same as during the registration period, especially for ongoing EEG biometrics that are free from sensory stimulation and tight cognitive control. The inter-state condition is to train and test a model using EEG collected in different states. It evaluates whether the model is capable of dealing with EEG signals in an unseen state, i.e., the inter-state stability capacity of a model.

The evaluation covers deep neural network-based methods, including multi-channel EEG timeseries + CNN, univariate features + CNN, functional connectivity networks + CNN, and a classic method using univariate features (with feature selection) and Mahalanobis classifier. Three types of univariate features, including band powers, AR coefficients, and fuzzy entropy, are extracted from each channel and concatenated into a feature vector. For calculation of EEG functional connectivity networks, correlation (COR) and phase synchronisation index (PSI) are selected based on previous results [5]. Their definitions will be given in the following section. For clarity, the methods being evaluated are referred to as Raw+CNN, Uni+CNN, Cor+CNN, PSI+CNN, and Uni+FS+Mah, respectively, as summarised in Table 2.

Table 2: Methods being evaluated

Methods	Input/ Features	Dimensions	Classifiers
Raw+CNN	Timeseries	$N_c \times N_s$	CNN
Uni+CNN	AR(4), FuzzEn, Band power(5)	$N_c \times 10$	CNN
Cor+CNN	FCN	$N_c \times N_c$	CNN
PSI+CNN	FCN	$N_c \times N_c$	CNN
Uni+FS+Mah*	Selected univariate features	1-D vector	Mahal. dist.

N_c and N_s denote the number of channels and signal sampling rate, respectively.
*For details about the feature extraction and selection, refer to Appendix A.

Data used for analysis is collected from the PhysioNet EEG motor movement and imagery (MMI) dataset [24]. This dataset contains EEG signals of 109 subjects in resting states and motor movement/imagery tasks. For each subject, we group these signals into four states: resting with eyes closed (EC), resting with eyes open (EO), physical motor movement (PHY), and motor imagery (IMA). Each state will be used for training and testing, resulting in a total of 16 training and testing scenarios, 4 of which are intra-state conditions and the rest are inter-state conditions. The signals were recorded from 64 electrodes with a sampling rate of 160 Hz, and were referenced to the earlobes. The signal preprocessing follows the common pipeline which comprises DC offset removal, bandpass filtering within [0.5 42] Hz, and artifact removal. Finally, a non-overlapping moving window of one second was used for generating training and testing samples, therefore, each sample is a one-second EEG segment. To analyse the impact of EEG channel density on biometric recognition, we test each method with four channel configurations where each of them corresponds to a portable EEG acquisition device: all 64 electrodes, the Cognionics QUICK-20 (blue), Cognionics QUICK-30 (blue+yellow), and EMOTIV EPOC+ (green), as illustrated in Fig. 1. Finally, a 5-fold cross-validation scheme is adopted in all experiments.

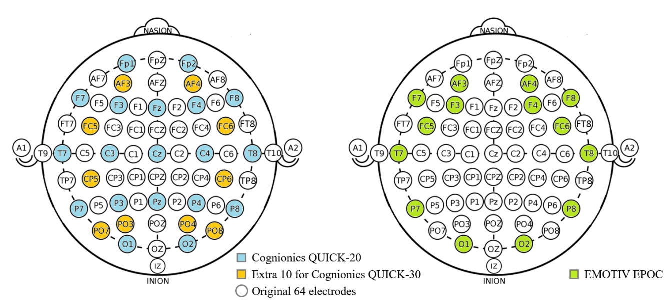

Fig. 1: Electrode placement and configurations

Fig. 2 reports the recognition performance of each method in the intra-state and inter-state conditions under the four channel configurations. The bar charts show the average CRR of all training and testing scenarios of each condition. For detailed results of each scenario and the significance test, please refer to Appendix B and Table 3-4 in Appendix C. Based on the results, the following observations are summarised. First, channel configuration has a significant impact on biometric recognition performance. Specifically, as the number of channels decreases, CRR shows a downward trend in both intra-state and inter-state test conditions. This trend is consistent for all methods, especially for methods using EEG functional connectivity.

For example, the decline in CRR of COR+CNN and PSI+CNN in Epoc+ configuration is larger than that of Raw+CNN and Uni+CNN methods. Second, EEG functional connectivity provides higher inter-state stability than univariate features and raw signals. For example, Raw+CNN and Uni+CNN achieved high CRR in the intra-state test conditions, however, their performance declined significantly in the inter-state test conditions. In contrast, COR+CNN and PSI+CNN outperformed Raw+CNN and Uni+CNN with All64 and Quick30 configurations in the inter-state test conditions. Although the CRR of COR+CNN and PSI+CNN dropped as the number of channels decreased, their potential of improving the inter-state stability is demonstrated. Third, as suggested by neuroimaging studies, EEG functional connectivity-based methods required a sufficient number of channels to support reliable analysis [25]. Our results show a similar trend that connectivity-based methods are susceptible to the number of channels. In addition, comparing results of the two conditions, a large inter-state variability within the same subject is observed, which indicates that the cognitive states of subjects have big impact on the identity-bearing patterns. Finally, the advantage of deep neural networks is demonstrated by comparing the results of CNN and results of Mahalanobis classifier.

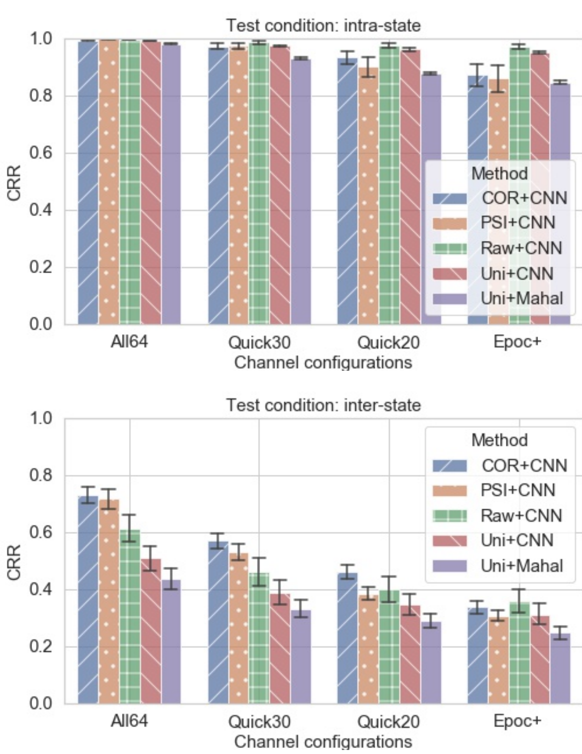

Fig. 2: Average CRR of intra-state and inter-state conditions under different channel configurations. The bars and error bars indicate the average and standard deviation.

In summary, EEG functional connectivity can potentially provide stable identity-bearing patterns for biometric recognition. However, a sufficient number of channels are needed to support stable performance. Therefore, a framework for reliable EEG biometrics with high CRR is proposed in this study.

4. Framework for reliable EEG biometrics

The proposed framework, as illustrated in Figure 3, consists of four modules, including a signal preprocessing module for data denoising and missing channel detection, a data augmentation module for density enhancement as well as missing channel reconstruction, a dynamic functional connectivity estimation module, and a deep learning module based on CNN, which extracts identity-bearing representations from the network inputs to support robust subject recognition.

4.1. Preprocessing

The signal preprocessing procedure adopted in the framework consists of the following steps: DC offset removal, band-pass filtering, missing channel detection, and artifact removal. Four types of artifacts are detected and corrected, including 1) channel artifacts (poor quality signals or erratic signals) due to bad contact or electrode mechanical faults; 2) epoch artifacts due to subject movement; 3) artifactual independent components which reflect ocular and muscular contamination; and 4) transient artifacts such as short bursts of white noise due to transient electrical faults or temporary poor contact. A thresholding method using statistical parameters of the data is used for artifact detection [26].

4.2. Density augmentation

The density augmentation module is designed for boosting the number of EEG channels collected by low density portable devices, as well as reconstructing missing channels or contaminated channels. The spherical spline interpolation is used [27]. It assumes a unit sphere for the scalp and projects the real scalp surface onto the sphere. Thus, any surface location can be represented as a vector emitted from the centre point of the sphere. This vector, can then be expressed by two angles θ and ϕ which denote the rotation from the x-axis towards the y-axis and the angular displacement from the x-y plane towards the z-axis, respectively, in spherical coordinate system.

Let $\mathbf{r}$ denote the location of an arbitrary point on the surface, with its potential as $V(\mathbf{r})$, and $\mathbf{r}_i$ denote the spherical projection location of electrode i, $i \in \{1, 2, \cdots, N_{ele}\}$. Then spherical spline interpolation assumes that the EEG potential at any point $\mathbf{r}$ on the surface of the sphere, $V(\mathbf{r})$, can be expressed as:

$$V(\mathbf{r}) = c_0 + \sum_{i=1}^{N_{ele}} c_i g_m(cos(\mathbf{r}, \mathbf{r}_i)) \tag{1}$$

where $c_0, c_1, \cdots, c_{N_{ele}}$ are constants fit to the data obtained by solving:

$$\sum_{j=1}^{N_{ele}} g_m(cos(\mathbf{r}_i, \mathbf{r}_j))c_j + c_0 = V(\mathbf{r}_i) \tag{2}$$

with a condition that:

$$\sum_{j=1}^{N_{ele}} c_j = 0 \tag{3}$$

where $V(\mathbf{r}_i)$ is EEG potential measured at electrode i, and $i, j \in \{1, 2, \cdots, N_{ele}\}$. The $cos(\mathbf{r}_i, \mathbf{r}_j)$ denotes the cosine of the angle

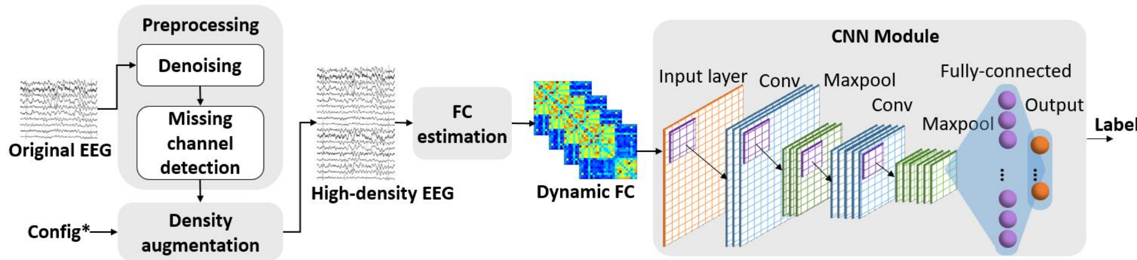

Fig. 3: Illustration of the framework. *A desired channel configuration.

between the two surface projection locations $\mathbf{r}_i$ and $\mathbf{r}_j$, which is given by:

$$cos(\mathbf{r}_i, \mathbf{r}_j) = \frac{\mathbf{r}_i \cdot \mathbf{r}_j}{|\mathbf{r}_i| \cdot |\mathbf{r}_j|} = 1 - \frac{(x_i - x_j)^2 + (y_i - y_j)^2 + (z_i - z_j)^2}{2} \quad (4)$$

where (x_i, y_i, z_i) and (x_j, y_j, z_j) are the Cartesian coordinates of surface projection of electrode i and j assuming a unit sphere. The function $g_m(x)$ is used for cosine distance and is given by:

$$g_m(x) = \frac{1}{4\pi} \sum_{n=1}^{N_{order}} \frac{(2n+1)P_n(x)}{n^m(n+1)^m} \quad (5)$$

where P_n is the Legendre polynomial of order n which defines the spatial harmonic frequencies, and m is a parameter that controls the spline flexibility. Computing $P_n(x)$ can be done through recurrent iteration according to:

$$(n+1)P_{n+1}(x) = (2n+1)xP_n(x) - nPn - 1(x) \quad (6)$$

with $P_0 = 1$ and $P_1 = x$. We set $m = 4$ and $N_{order} = 7$, as suggested by Perrin [27], to ensure sufficient precision on estimating $g(x)$ (10^{-6}) considering the electrode settings of our study.

4.3. Functional connectivity estimation

The functional connectivity estimation module is designed to capture the dynamic coupling relationship between brain regions (channels). Two connectivity metrics are selected based on a previous study [5] which are Pearson's correlation (COR) and phase synchronisation index (PSI).

Let x_i and x_j denote EEG signals from two different channels, respectively. The COR connectivity is given by:

$$COR(x_i, x_j) = \frac{1}{N_s} \sum_{k=1}^{N_s} x_i(k)x_j(k) \quad (7)$$

where N_s is the number of time points of the signals. The phase synchronisation measure is defined by the relative phase which is:

$$\Delta\phi_r(t) = |\phi_{x_i}(t) - \phi_{x_j}(t)| \mod 2\pi \quad (8)$$

where $\phi_x(t)$ denotes the instantaneous phase of signal $x(t)$ and it is calculated by applying Hilbert transform to the signal. Then the PSI measures how far the $Delta\phi_r(t)$ is deviated from a uniformly distributed phase using Shannon entropy, as follows:

$$RHO(x_i, x_j) = \frac{E(\text{uniform}) - E(\Delta\phi_r)}{E(\text{uniform})} \quad (9)$$

where $E(\cdot)$ denotes calculation of entropy and $E(\Delta\phi_r(t)) = -\sum_k p_k \ln(p_k)$ with the probability p_k approximated by generating a histogram of $\Delta\phi_r(t)$. The E(uniform) represents the maximum entropy of a uniform distribution. Considering the effect of the frequency content, the PSI is calculated on beta band EEG signals based on previous findings [5].

4.4. Learning EEG biometric identifiers

A convolutional neural network is designed to automatically learn inherent functional connectivity representations that exhibit unique identity-bearing patterns. The CNN cascades seven layers: Input ($N_c \times N_c$) - Conv (32, 4×4) - MaxPooling (2×2) - Conv (64, 4×4) - MaxPooling (2×2) - Dense (128) - Output. Specifically, in the convolutional layer, convoluted feature maps are extracted by local linear filters and work as parallel filters to detect the structural representations from the dynamic brain networks generated from functional connectivity estimation module. In addition, the max-pooling layer serves as a sub-sampling procedure that reduces the spatial dimensionality of each feature map while maintaining its discriminative identity-bearing characteristics.

The training procedure is based on iterating the cross entropy loss by the Adam optimiser. The initial learning rate is set to be 0.0005 and the batch size is 100. Meanwhile, batch normalisation is adopted before the convolution layer and the dense layer for accelerating the training speed. Furthermore, 25% dropout is applied after the max-pooling layers and the dense layer to reduce possible over-fitting. An early stopping strategy using a validation set made of 10% of the training data is also adopted to monitor over-fitting during the training stage. The error on the validation set is used as a proxy for the generalisation error in determining when over-fitting occurs.

5. Analysis and results

5.1. Density augmentation and stability

We first evaluate the impact of channel density augmentation on biometric performance. Fig. 4 reports the results of different methods with or without channel density augmentation. The two rows respectively show CRR results in the intra-state condition (specifically, signals of all states are mixed and split for training and testing) and inter-state condition (where resting-state EEG are used for training, and non-resting EEG are used for testing). The overall finding is that augmenting channel density improves biometric recognition performance,

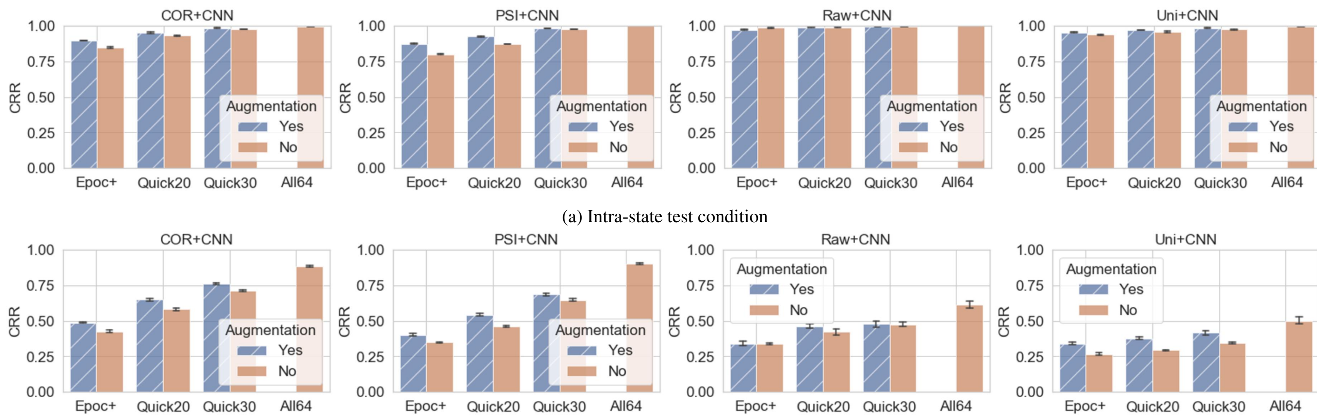

(a) Intra-state test condition

(b) Inter-state test condition

Fig. 4: The impact of channel density augmentation on biometric recognition. The average and standard deviation of the CRR results of the 5-fold cross-validation are reported. Results of the significance test are summarised in Appendix C.

especially the inter-state stability. Meanwhile, for different methods, electrode configurations, and test conditions, the enhancement brought by channel density augmentation varies.

Comparing results of each method with and without channel augmentation (each pair of blue bar and red bar), we can observe that channel density augmentation enhances CRR and this holds true for all the compared methods, electrode configurations and test conditions (except for Raw+CNN where the performance with and without augmentation is equivalent, that will be discussed later). Deep neural networks are data-driven models and having sufficient training data is important for the models to learn effective identity-bearing representations. As mentioned earlier, EEG data has two dimensions, i.e., the signal length and number of channels which affect the number of training samples and the dimension of each input. Previous studies have shown that obtaining a sufficient number of training samples through data augmentation can improve recognition performance, and our results demonstrate that having sufficient numbers of channels for the input through channel density augmentation can also facilitate the learning process.

Comparing results of each method under the two test conditions, we can see that the augmentation of channel density played an even greater role in the inter-state condition, indicating that having sufficient number of channels is important to maintain stable recognition performance in diverse human states. An input that contains richer information provides higher possibilities for the models to learn more robust identity-bearing representations.

Comparing results of the four methods, different degrees of enhancement can be observed. For the two functional connectivity-based methods, COR+CNN and PSI+CNN, channel augmentation substantially improved the CRR. For example, for COR+CNN in the inter-state condition, channel augmentation improved CRR by 6%, 7%, and 5% on average for the Epoc+, Quick20, and Quick30 configurations, respectively. The enhancement for Uni+CNN is also visible. However, for Raw+CNN, channel augmentation only achieved similar CRR equivalent to that of without channel augmentation. For example, results of the significance test in Table 5 in Appendix C show that, for Raw+CNN configured with Quick30, the difference between results of with and without augmentation is statistically insignificant. The same situation happened with Raw+CNN configured with Quick20 in the intra-state condition and Raw+CNN configured with Epoc+ in the inter-state condition. A possible explanation is that for raw EEG signals, channel density augmentation will introduce dependency among the input signals, which will affect the learning of neural networks. Therefore, directly training CNNs on the augmented EEG raw signals, i.e., Raw+CNN, will not necessarily improve CRR. However, the functional connectivity networks and univariate features extracted and established from the augmented raw signals are less sensitive to the impact of dependency between augmented raw signals. Instead, the augmented channels bring a richer input or feature set that may contain robust representations in different states. This is particularly true for functional connectivity-based methods, such as COR+CNN and PSI+CNN, where the number of channels have a large impact on the learning process, as discussed in Section 3.

In summary, the increase in channel density has a positive impact on biometric recognition performance. The improvement brought about by increased channel density is particularly prominent for COR+CNN and PSI+CNN. The results demonstrate that the proposed framework consisting of channel density augmentation, functional connectivity estimation and CNN is effective in enhancing the recognition accuracy and stability of EEG-based biometric systems. In addition, we partition the whole scalp area (64 channels) into four regions (frontal, central, parietal-occipital, and temporal) according to the cerebral cortex functions and analyse the contribution of each region. Results, in Appendix D, suggest that the frontal and central regions are strong biometric markers. Besides, the frontal area, especially the prefrontal area is superior in practical use since the preparation procedure is usually more convenient than the other regions and the forehead sensors are superb in terms of duration and ease of use.

5.2. *Volume conduction effects and biometric recognition*

We further evaluate the effect of volume conduction on EEG biometric recognition. Volume conduction describes the effects

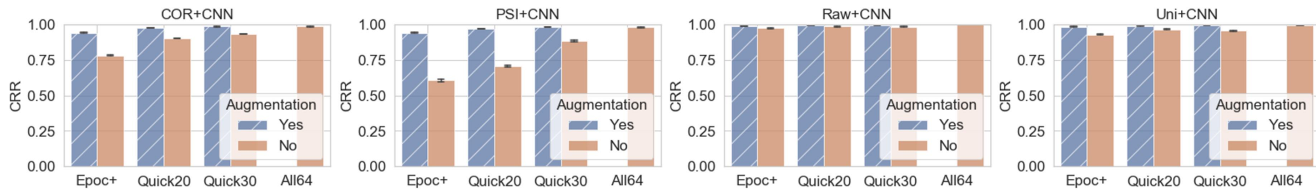

(a) Intra-state test condition

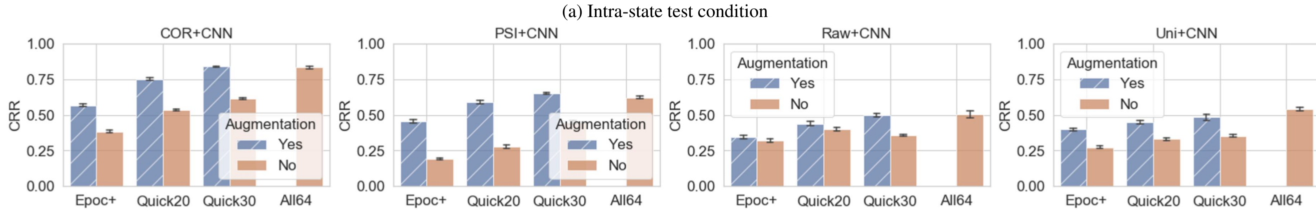

(b) Inter-state test condition

Fig. 5: The impact of channel density augmentation on biometric recognition - with surface Laplacian. The average and standard deviation of the CRR results of the 5-fold cross-validation are reported. Results of the significance test are summarised in Appendix C.

of recording electrical potentials at a distance from their source generator. For EEG signals recorded from the scalp surface, the volume conduction effects are generally high as each channel is a linear mixture of concurrently active brain and non-brain electrical sources whose activities are conducted to the scalp with broadly overlapping patterns [28]. On the one hand, this confounding effect can lead to spurious features, especially for connectivity estimates which measure the interaction between signals [28]. On the other hand, the volume conduction effect depends on the morphology and conductivity of the subject's head structure, which may contribute to the individual distinctiveness of the EEG signal [10]. Therefore, we apply surface Laplacian, to localise signals in order to study the impact of volume conduction effects on biometric applications.

The implementation of surface Laplacian in our framework follows Perrin's solution which is based on spherical spline interpolation due to its efficiency and high accuracy with few electrodes [27]. It is essentially a local operator based on the second spatial derivative of the potentials, as $\nabla^2_{surface}V(\mathbf{r})$. Considering the property of $P_n(x)$, we have:

$$\nabla^2_{surface}P_n = -(2n+1)P_n. \tag{10}$$

Then the current source density at $\mathbf{r}$, $D(\mathbf{r})$ can be estimated straightforwardly according to:

$$\nabla^2_{surface}V(\mathbf{r}) = \sum_{i=1}^{N_{ele}} c_i h_m(cos(\mathbf{r}, \mathbf{r}_i)) \tag{11}$$

with

$$h_m(x) = -\frac{1}{4\pi}\sum_{n=1}^{N_{order}} \frac{(2n+1)^2 P_n(x)}{n^m(n+1)^m}. \tag{12}$$

A smoothing parameter $\lambda = 10^{-5}$ is added to the diagonal of the g matrix when computing the current source density. The surface Laplacian reduces contributions of deep and distant sources and estimates current flow at each channel, thus, attenuating the potential volume conduction effects [29].

Fig. 5 reports the impact of channel density augmentation on biometric recognition for those methods with volume conduction effects reduced. The overall finding is consistent with that of Fig. 4, which is, augmenting channel density effectively improved recognition accuracy and inter-state stability. Not only that, the elimination of volume conduction effects even intensified the contribution of channel density enhancement in improving recognition accuracy and stability. For example, in the inter-state condition, for COR+CNN with surface Laplacian, channel augmentation improved CRR by 18%, 21%, and 22% on average for the Epoc+, Quick20, and Quick30 configurations, respectively. In contrast, in the same situation, for COR+CNN without surface Laplacian, the CRR improvement brought by channel augmentation is 6%, 7%, and 5%. The impact of volume conduction effects can be observed by comparing results in Fig. 4 and Fig. 5. A more direct comparison is presented in Appendix E. For inputs without channel density augmentation, eliminating the volume conduction effect reduces the CRR in most cases. This trend is consistent for different channel configurations and for both functional connectivity and signal timeseries inputs. The only exception is with univariate features, especially in the inter-state condition, where removing the volume conduction effect did not lead to a decrease of the CRR. Our results supports the hypothesis that the volume conduction effects which depend on the morphology and conductivity of the subject's head structure are also a contributing component to individual EEG distinctiveness. Therefore, by applying the surface Laplacian to reduce the volume conduction effects, some identity-bearing patterns that may contribute to biometric recognition are lost. As shown in the results, the confounding effects of volume conduction particularly affect scalp-based functional connectivity estimates, while for univariate features, the effect is small. On the other hand, for inputs after channel density augmentation, the opposite trend can be observed that surface Laplacian improves recognition accuracy. One explanation is that the density augmentation introduces dependencies between the signals which further introduces spatial autocorrelation that limits spatial precision and cause spurious connectivity [29]. The surface Laplacian, which can be viewed as a spatial filter, attenuates spatial autocorrelation, and thus improves the connectivity estimates.

6. Conclusion

This study evaluated the impact of channel density of EEG signals on biometric recognition, especially the inter-state stability. Results validated that insufficient density has a negative impact on recognition accuracy and inter-state stability. This is true for various methods regardless of the features and classifiers. Specifically, methods based on functional connectivity and deep learning show promising potential in improving inter-state stability, but the improvement is largely limited by the channel density. Therefore, a framework was proposed to augment EEG density to achieve high recognition accuracy as well as improving the inter-state stability. The framework supports reliable EEG biometric systems using low-density ongoing EEG collected by portable devices with sparse electrode settings, and thus facilitates flexible and practical uses. Results demonstrated that the framework dramatically improves the biometric recognition performance, especially in the inter-state scenarios. However, the proposed method is not suitable for systems with single electrode configurations because the spherical spline interpolation and functional connectivity estimation do need certain number of independent channels to support reliable estimates. Future study will focus on designing the optimal electrode configuration to achieve reliable EEG biometric systems of high usability and stability with minimum number of electrodes. In addition, we will further assess the framework in cross-session setups for a longitudinal evaluation [30] and extend the analysis scope to the authentication scenario.

Acknowledgements

This project is funded by an Australian Research Council Discovery Grant DP160102037.

References

[1] Q. Gui, M. V. Ruiz-Blondet, S. Laszlo, Z. Jin, A survey on brain biometrics, ACM Computing Surveys 51 (6) (2019) 112.

[2] M. Wang, H. El-Fiqi, J. Hu, H. A. Abbass, Convolutional neural networks using dynamic functional connectivity for EEG-based person identification in diverse human states, IEEE Transactions on Information Forensics and Security 14 (12) (2019) 3259–3272.

[3] P. Campisi, D. La Rocca, Brain waves for automatic biometric-based user recognition, IEEE Transactions on Information Forensics and Security 9 (5) (2014) 782–800.

[4] S. Yang, F. Deravi, S. Hoque, Task sensitivity in EEG biometric recognition, Pattern Analysis and Applications 21 (1) (2018) 105–117.

[5] M. Wang, J. Hu, H. A. Abbass, BrainPrint: EEG biometric identification based on analyzing brain connectivity graphs, Pattern Recognition 105 (2020) 107381.

[6] M. Fraschini, S. M. Pani, L. Didaci, G. L. Marcialis, Robustness of functional connectivity metrics for EEG-based personal identification over task-induced intra-class and inter-class variations, Pattern Recognition Letters 125 (2019) 49–54.

[7] S. Yang, F. Deravi, On the usability of electroencephalographic signals for biometric recognition: A survey, IEEE Transactions on Human-Machine Systems 47 (6) (2017) 958–969.

[8] E. Maiorana, D. La Rocca, P. Campisi, On the permanence of EEG signals for biometric recognition, IEEE Transactions on Information Forensics and Security 11 (1) (2015) 163–175.

[9] M. Abo-Zahhad, S. M. Ahmed, S. N. Abbas, A new multi-level approach to EEG based human authentication using eye blinking, Pattern Recognition Letters 82 (2016) 216–225.

[10] D. La Rocca, P. Campisi, B. Vegso, P. Cserti, G. Kozmann, F. Babiloni, F. D. V. Fallani, Human brain distinctiveness based on EEG spectral coherence connectivity, IEEE Transactions on Biomedical Engineering 61 (9) (2014) 2406–2412.

[11] W. Chen, Z. Wang, H. Xie, W. Yu, Characterization of surface EMG signal based on fuzzy entropy, IEEE Transactions on neural systems and rehabilitation engineering 15 (2) (2007) 266–272.

[12] T. C. Ferree, P. Luu, G. S. Russell, D. M. Tucker, Scalp electrode impedance, infection risk, and EEG data quality, Clinical Neurophysiology 112 (3) (2001) 536–544.

[13] P. L. Nunez, R. Srinivasan, A. F. Westdorp, R. S. Wijesinghe, D. M. Tucker, R. B. Silberstein, P. J. Cadusch, EEG coherency: I: statistics, reference electrode, volume conduction, laplacians, cortical imaging, and interpretation at multiple scales, Electroencephalography and clinical neurophysiology 103 (5) (1997) 499–515.

[14] W. Kong, Q. Fan, L. Wang, B. Jiang, Y. Peng, Y. Zhang, Task-free brainprint recognition based on degree of brain networks, in: Proceedings of the International Conference on Neural Information, Springer, 2017, pp. 709–717.

[15] M. Fraschini, A. Hillebrand, M. Demuru, L. Didaci, G. L. Marcialis, An EEG-based biometric system using eigenvector centrality in resting state brain networks, IEEE Signal Processing Letters 22 (6) (2015) 666–670.

[16] H. El-Fiqi, M. Wang, N. Salimi, K. Kasmarik, M. Barlow, H. Abbass, Convolution neural networks for person identification and verification using steady state visual evoked potential, in: Proceedings of the IEEE International Conference on Systems, Man, and Cybernetics (SMC), IEEE, 2018, pp. 1062–1069.

[17] H. Cecotti, A. Graser, Convolutional neural networks for P300 detection with application to brain-computer interfaces, IEEE Transactions on Pattern Analysis and Machine Intelligence 33 (3) (2011) 433–445.

[18] R. Das, E. Maiorana, P. Campisi, Visually evoked potential for EEG biometrics using convolutional neural network, in: Proceedings of the 25th European Signal Processing Conference (EUSIPCO), IEEE, 2017, pp. 951–955.

[19] L. Ma, J. W. Minett, T. Blu, W. S. Wang, Resting state EEG-based biometrics for individual identification using convolutional neural networks, in: Proceedings of the 37th Annual International Conference on Engineering in Medicine and Biology Society (EMBC), IEEE, 2015, pp. 2848–2851.

[20] Z. Mao, W. X. Yao, Y. Huang, EEG-based biometric identification with deep learning, in: Proceedings of the 8th International IEEE/EMBS Conference on Neural Engineering (NER), IEEE, 2017, pp. 609–612.

[21] L. Chu, R. Qiu, H. Liu, Z. Ling, X. Shi, Individual recognition in schizophrenia using deep learning methods with random forest and voting classifiers: Insights from resting state EEG streams, arXiv preprint arXiv:1707.03467 (2017) 1–7.

[22] S. M. Abdelfattah, G. M. Abdelrahman, M. Wang, Augmenting the size of EEG datasets using generative adversarial networks, in: 2018 International Joint Conference on Neural Networks (IJCNN), IEEE, 2018, pp. 1–6.

[23] H. El-Fiqi, M. Wang, K. Kasmarik, A. Bezerianos, K. C. Tan, H. A. Abbass, Weighted gate layer autoencoders, IEEE Transactions on Cybernetics (2021) 1–12.

[24] A. L. Goldberger, L. A. Amaral, L. Glass, J. M. Hausdorff, P. C. Ivanov, R. G. Mark, J. E. Mietus, G. B. Moody, C. K. Peng, H. E. Stanley, Physiobank, physiotoolkit, and physionet, Circulation 101 (23) (2000) e215–e220.

[25] C. M. Michel, M. M. Murray, Towards the utilization of EEG as a brain imaging tool, Neuroimage 61 (2) (2012) 371–385.

[26] H. Nolan, R. Whelan, R. B. Reilly, FASTER: fully automated statistical thresholding for EEG artifact rejection, Journal of neuroscience methods 192 (1) (2010) 152–162.

[27] F. Perrin, J. Pernier, O. Bertrand, J. Echallier, Spherical splines for scalp potential and current density mapping, Electroencephalography and clinical neurophysiology 72 (2) (1989) 184–187.

[28] C. Brunner, M. Billinger, M. Seeber, T. R. Mullen, S. Makeig, Volume conduction influences scalp-based connectivity estimates, Frontiers in computational neuroscience 10 (2016) 121.

[29] M. X. Cohen, Surface Laplacian, in: Analyzing neural time series data: theory and practice, MIT press, 2014, pp. 275–289.

[30] E. Maiorana, P. Campisi, Longitudinal evaluation of EEG-based biometric recognition, IEEE Transactions on Information Forensics and Security 13 (5) (2017) 1123–1138.

Appendix A Details of method Uni+FS+Mahal

Three types of univariate features are extracted from each channel, including 5 average band power features, 4 AR coefficient features, and 1 fuzzy entropy feature. Specifically, the Welch's method, a nonparametric method based on Fourier transform, is used for estimation of the power spectral density, and the averaged power of the five EEG canonical frequency bands (i.e., delta, theta, alpha, beta, and gamma) are computed as features. Moreover, an AR model of order 4 is estimated using the Burg method and the polynomial coefficients are used as features. Furthermore, the fuzzy entropy [11] of each channel is calculated. Finally, the three types of univariate features are concatenated into a feature vector of 10 features per channel.

The minimum redundancy maximum relevance algorithm (MRMR) is used for feature selection. It finds a subset of features that is mutually far away from each other (i.e., minimum redundancy) while representing the response variable effectively (i.e., maximum relevance). Classification is based on the Mahalanobis distance discriminant model which has been widely used for EEG biometric systems for its high efficiency [10, 5]. Given a small number of training samples for a class (subject), the covariance matrix of the feature vectors of the class may not be robustly estimated. Thus, a pooled covariance matrix, C, is estimated using the whole training set to approximate the class-specific covariance matrices. In addition, a mean feature vector $\mathbf{u}_m$ is computed for each class. In the test phase, for a query sample $\mathbf{v}_o$, its Mahalanobis distances to each class, $d_{o,m}$, is calculated and the label of the class that achieves the minimum distance is the output prediction, as follows:

$$d_{o,m} = (\mathbf{v}_o - \mathbf{u}_m)\mathbf{C}^{-1}(\mathbf{v}_o - \mathbf{u}_m)^T \tag{13}$$

$$\hat{o} = argmin_m(d_{o,m}). \tag{14}$$

Given a training set, we rank all features in the set in descending order of importance using the MRMR algorithm. Fig. 6 reports the CRR of Uni+FS+Mahal method when using different numbers of top-ranked features. The first row visualises the results for different channel configurations in the intra-state test conditions. The second and third rows visualise the results for different channel configurations in the inter-state test conditions. The number of features is $10 \cdot N$, where N is the number of channels. Therefore, for the four channel configurations, i.e., All64, Quick30, Quick20, and Epoc+, there are 640, 290, 190, and 140 features in total, respectively, before feature selection. For splitting the training and testing sets, a 5-fold cross validation scheme is adopted. Fig. 7 shows the top channels corresponding to the channel configuration, state of the training data, and run index (1-5 for 5-fold cross-validation).

From Fig. 6, we can observe that the CRR improves as the number of features increases, except in a few cases where CRR converges before the maximum number of features is reached. In addition, compared with intra-state test conditions, the significant drop in CRR under inter-state conditions further confirmed the large intra-subject variations due to state changes, especially between the resting states (EO and EC) and non-resting states (PHY and IMA). Finally, Fig. 7 indicates that the important channel and feature sets variate for different states, and they are even not consistent for different runs of the same state. Considering the differences in feature orders in different states, the optimal feature set that achieves the highest CRR is the full feature set. Therefore, the results of using the full feature set are reported for method Uni+FS+Mah in the main text.

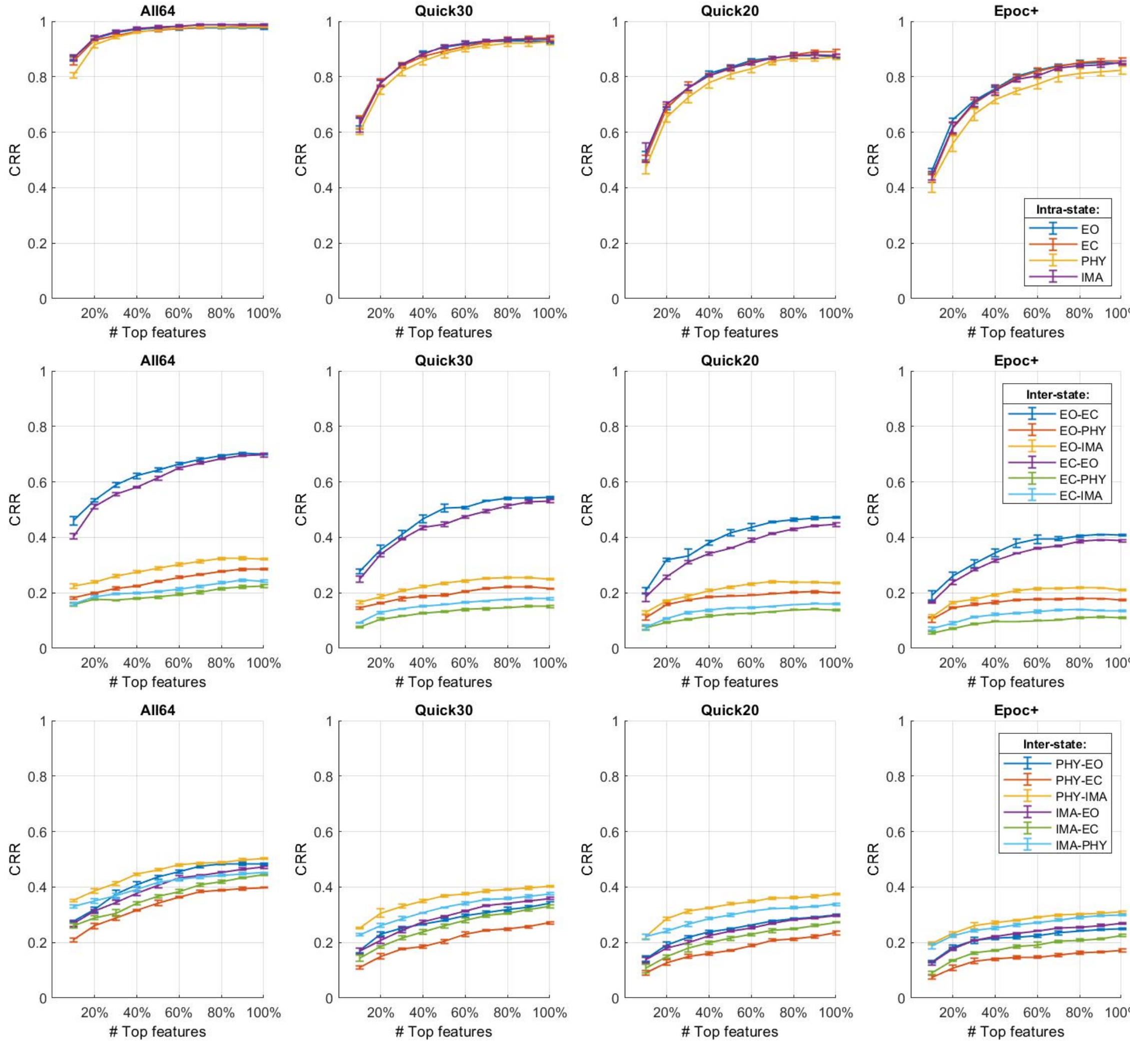

Fig. 6: Subject identification results of Uni+FS+Mahal. Each figure shows the change of CRR against the number of top features. The row and column represent the different test conditions and channel configurations, respectively. The line and error bar indicate the average and the standard deviation of the 5-fold cross-validation runs, respectively.

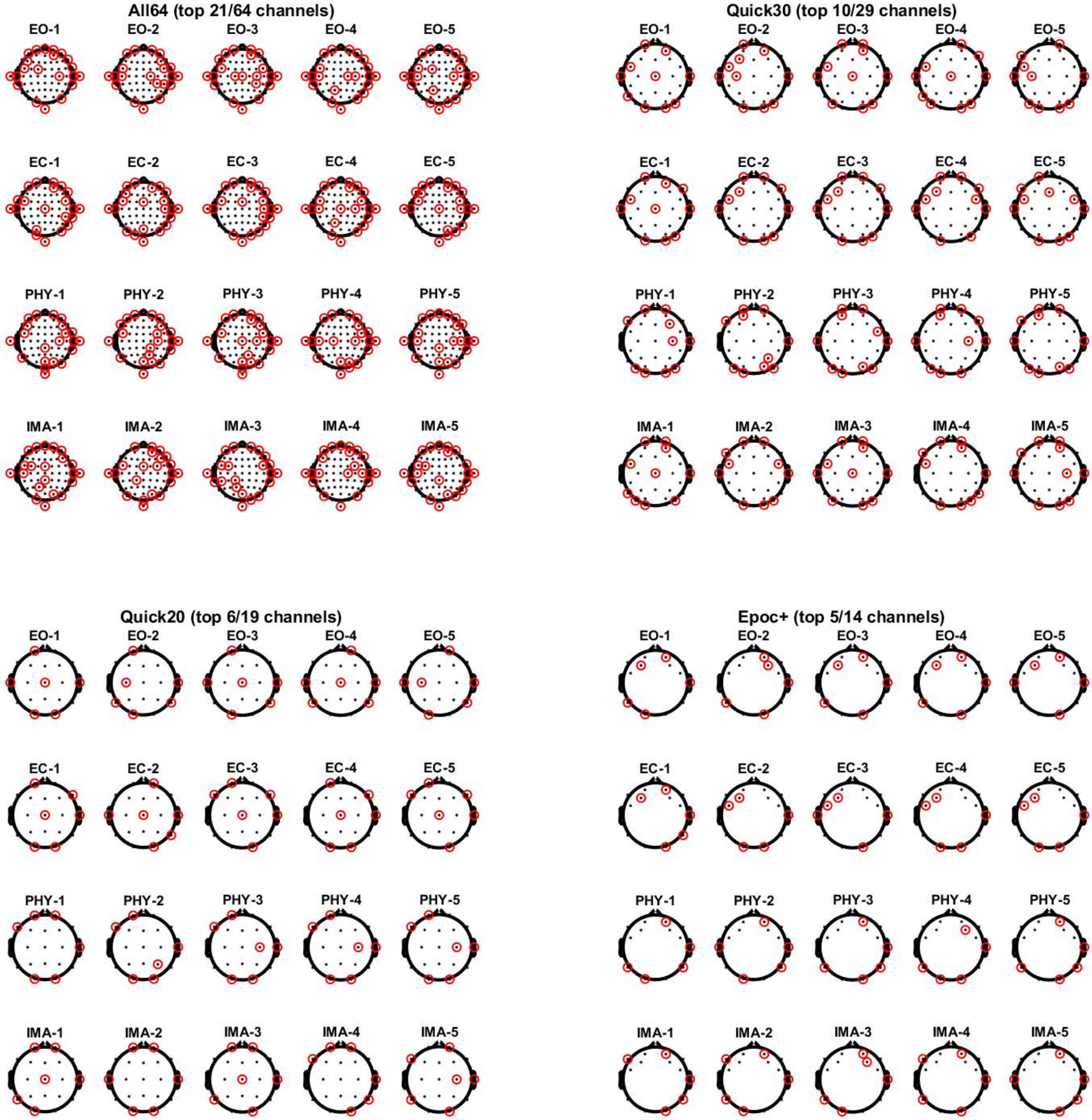

Fig. 7: Scalp locations of the channels of the top-ranked features. The black dots indicate channel configurations and the red circles indicate the channels of the top-ranked features. The numbers in the subtitles represent the cross validation runs.

Appendix B Detailed results for Section 3

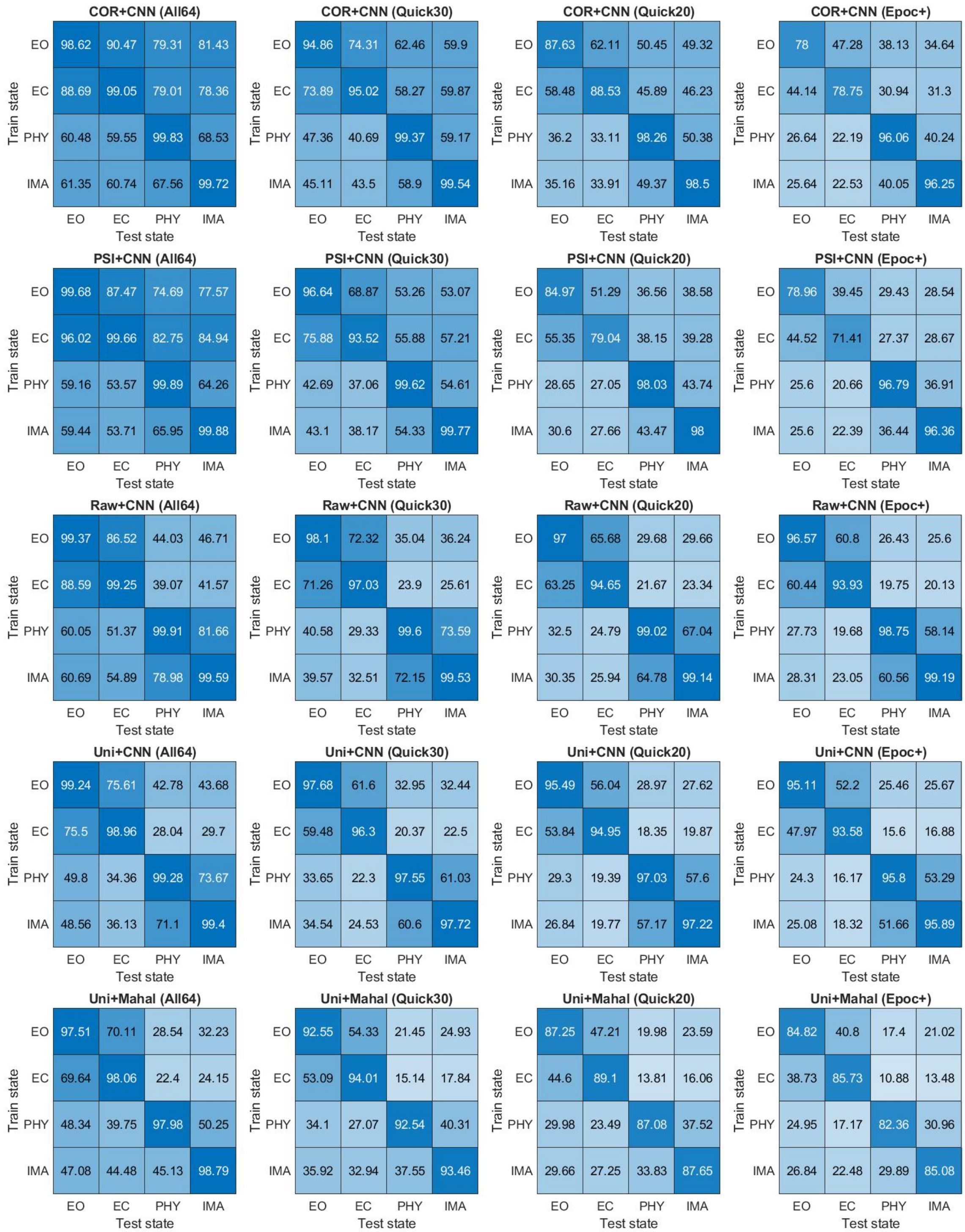

Fig. 8: Detailed CRR results for each training and testing state of the intra-state and inter-state conditions under different channel configurations.

Appendix C Significance test results

Table 3: Significance test for results in Fig. 2 - P values between results of different methods in each channel configuration.

Intra-state test condition							Inter-state test condition						
		COR+CNN	PSI+CNN	Raw+CNN	Uni+CNN	Uni+Mahal			COR+CNN	PSI+CNN	Raw+CNN	Uni+CNN	Uni+Mahal
All64	COR+CNN	-	6.80E-04*	8.20E-02	5.20E-01	1.10E-09*	All64	COR+CNN	-	1.40E-01	1.20E-05*	1.80E-13*	1.80E-19*
	PSI+CNN	-	-	8.70E-04*	8.80E-08*	2.80E-11*		PSI+CNN	-	-	2.80E-04*	3.70E-11*	2.40E-16*
	Raw+CNN	-	-	-	4.10E-04*	1.50E-09*		Raw+CNN	-	-	-	6.40E-20*	1.50E-25*
	Uni+CNN	-	-	-	-	1.90E-08*		Uni+CNN	-	-	-	-	6.20E-07*
Quick30	COR+CNN	-	5.10E-01	4.20E-04*	8.10E-01	1.60E-06*	Quick30	COR+CNN	-	2.40E-14*	1.70E-06*	5.80E-16*	6.70E-22*
	PSI+CNN	-	-	4.10E-03*	8.90E-01	7.20E-06*		PSI+CNN	-	-	1.40E-03*	8.40E-12*	1.20E-18*
	Raw+CNN	-	-	-	2.10E-05*	4.00E-11*		Raw+CNN	-	-	-	1.80E-19*	5.90E-13*
	Uni+CNN	-	-	-	-	4.60E-11*		Uni+CNN	-	-	-	-	4.40E-06*
Quick20	COR+CNN	-	1.50E-03*	1.20E-04*	7.60E-03*	4.40E-04*	Quick20	COR+CNN	-	1.60E-26*	1.40E-03*	1.90E-10*	9.20E-20*
	PSI+CNN	-	-	8.60E-05*	1.70E-03*	2.90E-01		PSI+CNN	-	-	3.60E-01	7.20E-03*	4.60E-12*
	Raw+CNN	-	-	-	1.00E-04*	3.20E-12*		Raw+CNN	-	-	-	1.60E-17*	8.30E-11*
	Uni+CNN	-	-	-	-	3.60E-14*		Uni+CNN	-	-	-	-	8.30E-06*
Epoc+	COR+CNN	-	1.20E-01	1.10E-05*	5.90E-04*	2.40E-01	Epoc+	COR+CNN	-	5.30E-11*	1.50E-01	3.50E-02*	1.30E-13*
	PSI+CNN	-	-	3.40E-05*	8.90E-04*	6.20E-01		PSI+CNN	-	-	6.40E-04*	6.30E-01	1.80E-10*
	Raw+CNN	-	-	-	3.30E-05*	8.20E-13*		Raw+CNN	-	-	-	3.70E-14*	1.10E-11*
	Uni+CNN	-	-	-	-	2.80E-14*		Uni+CNN	-	-	-	-	1.30E-07*

** Significance at level 0.05.*

Table 4: Significance test for results in Fig. 2 - P values between results of different channel configurations for each method.

Intra-state test condition						Inter-state test condition					
		All64	Quick30	Quick20	Epoc+			All64	Quick30	Quick20	Epoc+
COR+CNN	All64	-	7.60E-05*	2.00E-05*	6.10E-06*	COR+CNN	All64	-	1.90E-33*	2.80E-43*	2.00E-45*
	Quick30	-	-	1.30E-05*	3.50E-06*		Quick30	-	-	1.10E-40*	7.40E-46*
	Quick20	-	-	-	2.70E-06*		Quick20	-	-	-	8.80E-43*
PSI+CNN	All64	-	4.80E-04*	5.10E-05*	2.40E-05*	PSI+CNN	All64	-	6.50E-29*	7.10E-36*	2.80E-36*
	Quick30	-	-	2.40E-05*	1.20E-05*		Quick30	-	-	4.10E-38*	8.80E-37*
	Quick20	-	-	-	3.80E-06*		Quick20	-	-	-	5.00E-29*
Raw+CNN	All64	-	2.90E-04*	3.50E-05*	5.50E-05*	Raw+CNN	All64	-	4.20E-27*	6.00E-33*	4.70E-38*
	Quick30	-	-	8.70E-05*	1.30E-04*		Quick30	-	-	1.80E-18*	2.20E-26*
	Quick20	-	-	-	5.30E-02		Quick20	-	-	-	1.90E-16*
Uni+CNN	All64	-	6.80E-11*	8.40E-11*	7.90E-13*	Uni+CNN	All64	-	1.00E-34*	8.60E-37*	5.90E-39*
	Quick30	-	-	7.50E-06*	5.40E-11*		Quick30	-	-	1.50E-24*	1.00E-35*
	Quick20	-	-	-	2.70E-05*		Quick20	-	-	-	8.40E-23*
Uni+Mahal	All64	-	4.00E-16*	4.80E-20*	1.80E-19*	Uni+Mahal	All64	-	1.40E-31*	5.80E-28*	1.60E-29*
	Quick30	-	-	2.10E-19*	1.60E-18*		Quick30	-	-	7.30E-19*	3.70E-26*
	Quick20	-	-	-	4.20E-10*		Quick20	-	-	-	7.10E-29*

** Significance at level 0.05.*

Table 5: Significance test for results in Fig. 4 and Fig.5 - P values between results of the method with augmentation and without augmentation.

For results in Fig. 4.

	Intra-state test condition				Inter-state test condition			
	COR+CNN	PSI+CNN	Raw+CNN	Uni+CNN	COR+CNN	PSI+CNN	Raw+CNN	Uni+CNN
Quick30	3.90E-02*	8.20E-04*	4.70E-01	4.70E-02*	2.60E-05*	1.00E-05*	8.90E-01	3.90E-05*
Quick20	8.90E-04*	4.70E-06*	9.00E-01	8.20E-03*	1.70E-05*	8.00E-10*	3.00E-02*	4.00E-07*
Epoc+	7.30E-06*	3.90E-05*	1.50E-03*	5.00E-03*	1.90E-07*	6.20E-06*	9.60E-01	3.50E-07*

For results in Fig. 5

	Intra-state test condition				Inter-state test condition			
	COR+CNN	PSI+CNN	Raw+CNN	Uni+CNN	COR+CNN	PSI+CNN	Raw+CNN	Uni+CNN
Quick30	3.40E-07*	3.90E-06*	9.20E-04*	7.60E-05*	5.70E-12*	2.00E-11*	1.10E-08*	9.80E-09*
Quick20	4.90E-07*	7.90E-08*	1.70E-03*	1.00E-04*	4.70E-13*	2.20E-14*	3.90E-03*	5.60E-11*
Epoc+	2.20E-08*	2.20E-08*	1.70E-03*	2.30E-04*	3.50E-11*	3.10E-13*	8.30E-03*	6.00E-09*

** Significance at level 0.05.*

Appendix D Analysis on scalp regions

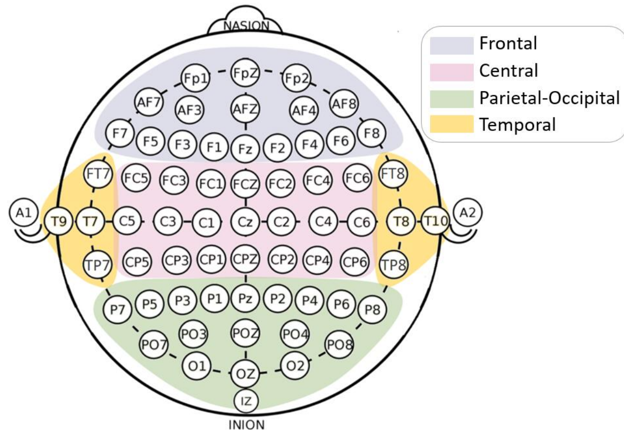

Fig. 9: Scalp electrode partitions.

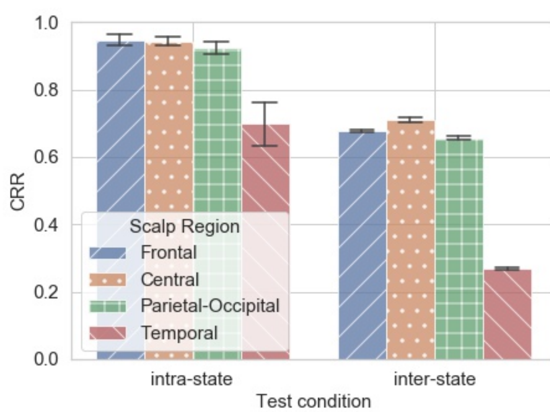

Fig. 10: CRR results for COR+CNN method using different scalp regions under intra-state and inter-state test conditions. The bars and error bars indicate the average and standard deviation of the results of the 5-fold cross-validation.

Appendix E The impact of volume conduction effects on biometric recognition

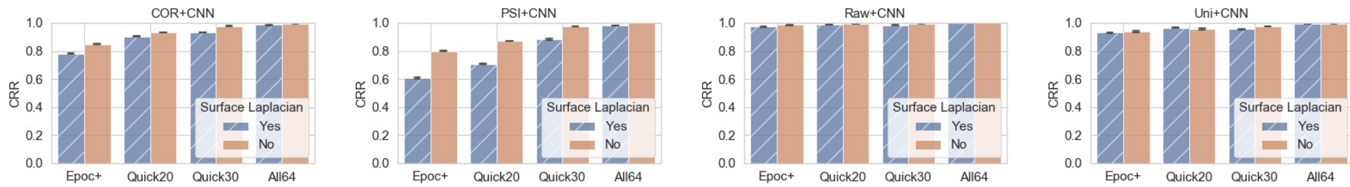

(a) Intra-state test condition

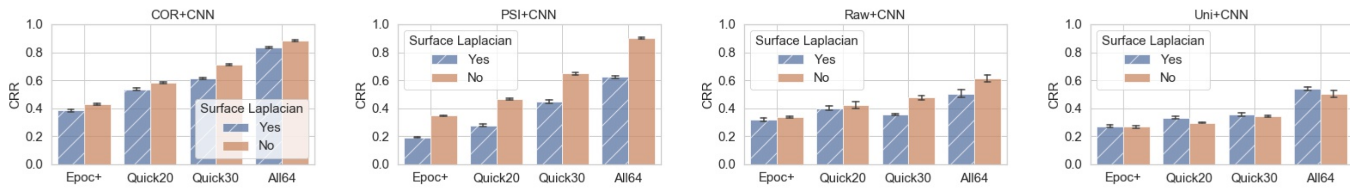

(b) Inter-state test condition

Fig. 11: The impact of reducing the volume conduction effects on biometric recognition - without channel density augmentation. The average and standard deviation of the CRR results of the 5-fold cross-validation are reported.

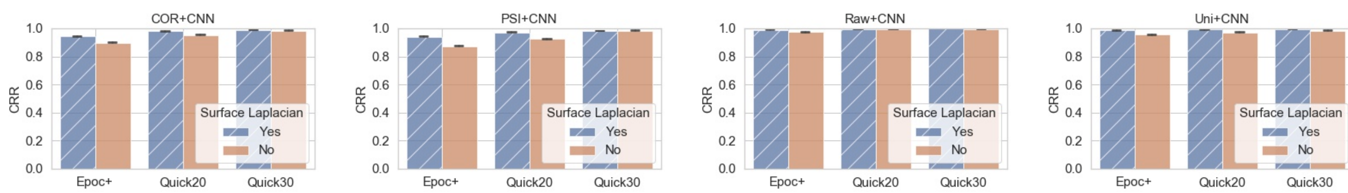

(a) Intra-state test condition

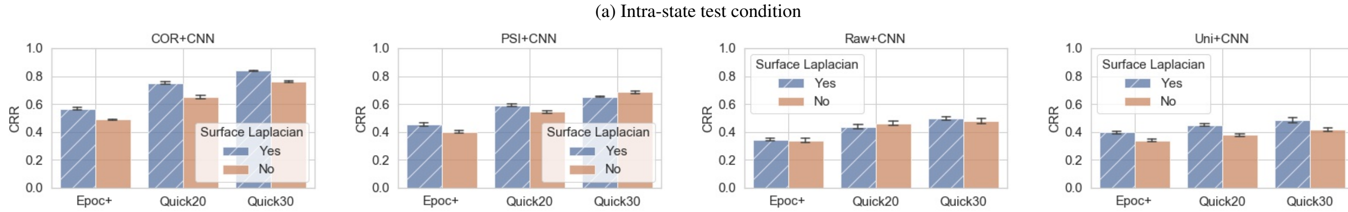

(b) Inter-state test condition

Fig. 12: The impact of reducing the volume conduction effects on biometric recognition - with channel density augmentation. The average and standard deviation of the CRR results of the 5-fold cross-validation are reported.